Integrity Provision for Map-Matched Positioning of Road Vehicles at Lane Level

Rafael Toledo-Moreo, David Betaille, François Peyret

Proceedings of the 12th International IEEE Conference
on Intelligent Transportation Systems, St. Louis, MO,
USA, October 3-7, 2009

Integrity Provision for Map-Matched Positioning of Road Vehicles at Lane Level

Rafael Toledo-Moreo *IEEE member*, David Bétaille *IEEE member* and François Peyret

***Abstract*— Many road safety applications and those with critical performance restrictions (such as satellite based electronic fee collection) demand from the onboard navigation systems, on the one hand, positions referred to a local map, and on the other hand, an indicator of the quality of these positions, the so called integrity. The map-matched positions are commonly estimated in two separated phases: firstly, position is determined by means of GNSS (in occasions assisted by odometry or inertial sensors) and secondly, a map-matching process is performed based on the position estimated previously. However, current common integrity indicators, imported from the aerial domain, only represent the quality of the GNSS input, and not the final combined map-matched position. The influence of the information coming from other sensors and maps is neglected, with negative consequences in the coherence between positioning and integrity. This paper presents a solution to the problem of integrity provision in a combined positioning and map-matching process, based on two complementary integrity parameters. To the best of the authors' knowledge, this is the first work that presents integrity monitoring of the complete navigation process, unifying both map-matching and positioning. Our proposal has been tested in real experiments in Germany, proving the validity of the concept, and its suitability to the problem under consideration.**

I. INTRODUCTION

Navigation systems are an essential part of a great number of ITS (Intelligent Transportation Systems) applications dedicated to improve the safety or efficiency of road traffic. While many applications can be satisfied by current GNSS (Global Navigation Satellite Systems) receivers, such as the most common in-car navigators or non-critical fleet management, some other applications demand a higher performance from the onboard navigation units. This is the case of safety applications or, for example, an Electronic Fee Collection (EFC) system that must rely on the navigation solution (GNSS or assisted GNSS) [1]. A good example of these new requirements is the increasing interest of the navigation at the lane level, with applications such as enhanced driver awareness (EDA), intelligent speed alert or simply lane allocation [2].

The needs of the new "high-demanding" applications can be threefold like next:

1) accurate positioning,
2) an accurate reference for the positioning that can be shared among users (an enhanced map or Emap), and
3) an indicator of the level of reliability that the user can have on the provided pose estimation (navigation integrity).

R. Toledo-Moreo is with the University of Murcia, Dept. of Information and Communication Engineering and with the Technical University of Cartagena, Dept. of Electronics and Computer Technology. D. Bétaille and F. Peyret are with the Laboratoire Central de Ponts et Chausses, LCPC Nantes Centre. toledo@um.es, david.betaille@lcpc.fr, francois.peyret@lcpc.fr

Let us now analyze these three aspects in further detail.

To achieve better accuracy and maintain it even during the outages of visibility of the GNSS satellites, the most common GPS (Global Positioning System) receiver can be assisted by SBAS (Satellite Based Augmentation Systems), such as EGNOS (European Geostationary Navigation Overlay System) in Europe, the Russian GLONASS (Global Navigation Satellite System) and/or odometry and inertial sensors [8].

Regarding maps, unfortunately currently available commercial maps present serious lacks of accuracy, contents and completeness to be applicable in high-demanding applications. This issue was previously addressed by the authors in [4]. In this paper it was shown how to create an Emap capable to meet the necessary completeness and accuracy restrictions. Some other approaches to this problem can be found in [5], [6].

Finally, integrity parameters for road navigation have been imported from the aerial domain despite the fact that many of the assumptions valid in the air are not verified in road scenarios [7]. The very different conditions of satellite visibility or multipath effects demand a reconsideration of the integrity concept for roads [3]. Furthermore, except for the case of car navigation on an absolutely unknown environment with no roads, the vehicle position must be referred to maps. Therefore, unlike in the aerial domain, new integrity indicators must cope with a map-matching process. Although there are attempts in the literature to provide integrity values for map-matching techniques [9], to the best of our knowledge, there is no reference of common integrity provision for both positioning and map-matching.

This paper presents a solution to the problem of providing an integrity estimate that represents map-matched positions, taking into account all the sensors of the navigation unit and the information about the road shape and topology stored in a enhanced map. Both positioning and map-matching are performed simultaneously by means of a single data-fusion process based on a particle filter (PF), and employing the measurements coming from a GNSS receiver, a gyroscope, the odometry of the vehicle, and an enhanced map (Emap) that describes the road as linked lane segments. In our proposal, we do not perform the common projection of the estimated position on the most likely road segment, but a straightforward single process that employs the information about the road shape and topology stored in the map as an observation vector in the filtering process. The output of the

978-1-4244-5521-8/09/$26.00 ©2009 IEEE

PF is a position within the bounds of the road segment in which the vehicle is allocated. Embedded in the filtering process, the calculation of the integrity of a map-matched position is based on the double representation of the location information, and given by two parameters:

- Firstly, a level of reliability on the road segment allocation (a probability value). Since in our Emap road is described by lanes, the integrity indicator consequently refers to the lane assignments, something that to the authors' knowledge, has not been addressed in the literature yet.
- Secondly, a level of confidence on the estimated position (in the way of a protection level value in meters). This value is based not only on GNSS measurements, as traditional RAIM (Receiver Autonomous Integrity Monitoring) based techniques do, but on the combination of all the sources of information employed in the positioning process, including of course the road map.

The rest of the paper is organized as follows: Sections II and III show respectively brief descriptions of our Emap paradigm and the most significant aspects of the positioning cycle. Our approach for integrity is described in Section IV. Section V shows the results obtained in terms of integrity provision, and main conclusions are drawn in Section VI.

II. EMAP DESCRIPTION

Most geographical information systems (GIS) represent roads with polylines, i.e. series of nodes and shape points, connected by straight segments. These simplifications lead to errors in map-matching and make unfeasible some applications such as those at lane level accuracy. The Emap that was presented in [4] describes road lanes as clothoids horizontally, as well as straight lines vertically. The proposed clothoid model may degenerate into circles or straight lines when needed, by adjusting shape parameters of the clothoid: zeroing the rate of curvature for circles and zeroing as well the initial curvature for straight lines. This approach fits well with the way roads are actually built [10]. [4] suggests a Kalman based extraction process, where generalized clothoid parameters are identified. Extended Kalman filters (EKF) smoothed GPS and dead-reckoning vehicle trajectories. Maximum deviation between the extracted geometry and the vehicle location was bounded to 5 cm. When the inclusion of a new point in a given segment causes that the distance between the most suitable clothoid and two points included in that clothoid become larger than 5 cm, the segment stops and a new clothoid starts with the new point. That way, the Emap meets the requirements of ITS applications for positioning and mapping at lane level accuracy.

In addition to the road shape, topological information is also included in our Emap. Every clothoid is analyzed in order to list its neighbors, and define whether these are front, left or right. This information speeds up the process of map-matching since the list of possible lane segments after leaving the current one is topologically constrained. A set of geometrical rules has been designed to interconnect automatically the segments and create the topological description of the road. More information about this process can also be found in [4].

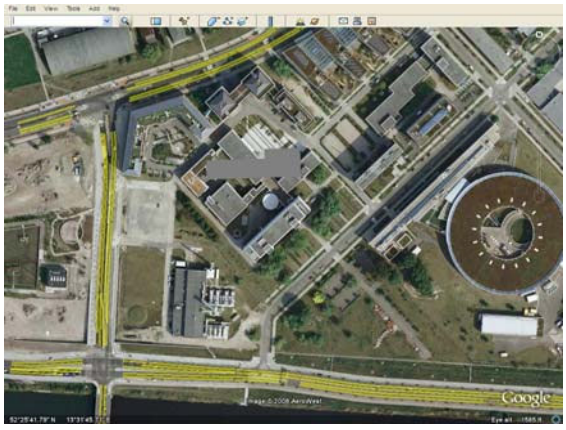

Fig. 1. Emap of Berlin test site superimposed to the Google Maps image of the area.

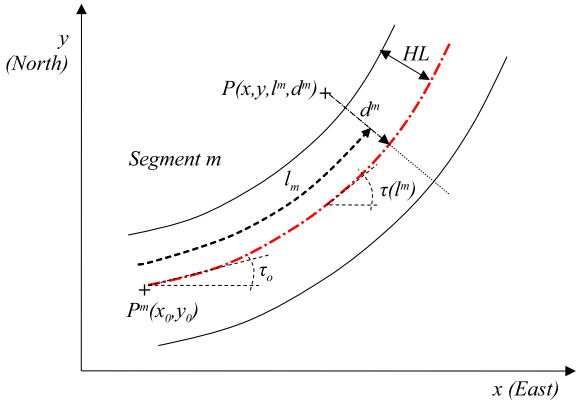

Fig. 2. Cartesian x, y and Frenet l^m, d^m coordinates for a point P, position of a vehicle driving segment m with a given half lane width HL. Initial angle of the segment τ_0, and angle at any Frenet abscissa $\tau(l_m)$.

Fig. 1 shows the Emap generated near Berlin Adlershof DLR test site.

III. POSITIONING CYCLE

The positioning loop, that is based on a particle filter, is shown in Fig. 3. Apart from the usual stages of initialization, prediction and normalization there are two steps of update, whether with Emap, or with GNSS observations. The nature of these observations encourages the use of a double reference system: the standard 2D global navigation frame (east, north), and a local frame that refers to the lane to which the vehicle position is assigned.

The state vector of our filter is a composition of a Cartesian and a Frenet sub-states, $\mathbf{X} = [\mathbf{X}^C, \mathbf{X}^F]$, where $\mathbf{X}^C$ stands for the Cartesian part and $\mathbf{X}^F$ for the Frenet one (in the following, these superscripts will be used to distinguish both sub-systems). $\mathbf{X}^C$ is defined by $[x, y, \psi]$, representing

East, North and heading angle respectively at the point of the GNSS antenna, while $\mathbf{X}^F$ includes $[l^m, d^m, m]$, that represent the values of abscissa and ordinate referred to the lane segment m. The state variables of the proposed filter are represented in Fig. 2.

The inclusion of Cartesian and Frenet definitions for the same point introduces a partial redundancy in the state vector, which implies some particularities in the implementation of the particle filter. On the other hand, it brings some benefits to its implementation:

- Frenet variables are more adequate for evaluating the transitions between lane segments of the road, and applying Emap observations.
- East, North values for positioning are necessary in a number of location based services. In addition to that, the inclusion of a Cartesian sub-state allows uninterrupted navigation also when the Emap reference is not present.

The state vector that represents a particle i at instant k according to the variables presented in Fig. 2 is given by

$$X_k^i = [x_k^i, y_k^i, \psi_k^i, l_k^{m,i}, d_k^{m,i}, m_k^i] \tag{1}$$

Both Frenet and Cartesian representations of the same point are related by the expression

$$\begin{aligned} x &= x_0^m + \int_0^{l^m} cos(\tau^m(l^m))dl \quad - d^m sin(\tau^m(l^m)) \\ y &= y_0^m + \int_0^{l^m} sin(\tau^m(l^m))dl \quad + d^m cos(\tau^m(l^m)) \end{aligned} \tag{2}$$

where x_0^m, y_0^m are the East and North coordinates of the initial point of the road segment and $\tau^m(l^m)$ is the azimuth angle of the segment at abscissa l^m, given by

$$\tau^m(l^m) = \tau_0^m + \kappa_0^m \cdot l^m + \frac{c^m \cdot (l^m)^2}{2}. \tag{3}$$

being τ_0^m, κ_0^m and c^m shape parameters of the clothoid definition of segment m, and representing initial heading, initial curvature, and linear curvature rate respectively (Fig. 2).

Further details of the positioning cycle can be found in [11].

IV. INTEGRITY DEFINITION

The proposed definition of integrity for the problem under consideration embraces:

1) the capability of the system to identify correctly the lane segment on which the vehicle is at every epoch, detecting possible mismatches in the segment assignment, and
2) to estimate accurately the vehicle position on that lane with relevant confident indication.

Consequently, the integrity level of the map-matched position of the vehicle is represented by two variables, explained next.

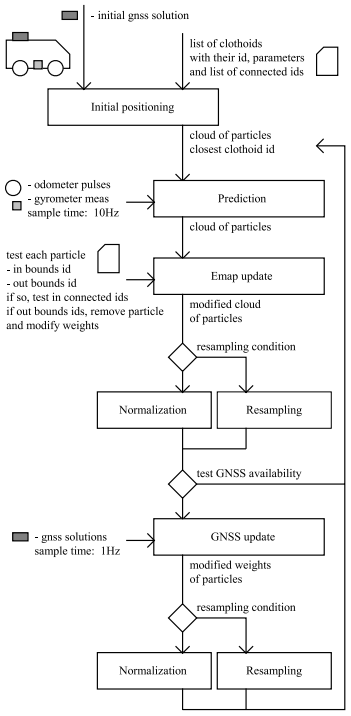

Fig. 3. Flowchart of the single positioning and map-matching fusion process.

A. Lane Occupancy Probability (μLO)

The probability that the vehicle occupies lane segment r at instant k, $\mu_k^{m=r}$, can be calculated as the addition of the normalized weights of particles that are associated to segment r, following next expression:

$$\mu_k^{m=r} = \sum_{i=1}^{N} w_k^{i|m=r} \tag{4}$$

Let us remark that since both positioning and map-matching are performed simultaneously by our filter, this parameter is representative of the level of confidence of both navigation operations. Indeed, the weight of a particle i at instant k, w_k^i, depends on the prediction obtained by employing the inputs of odometry and gyroscope to the vehicle model, on the road information applied in the Emap update phase, and finally on the GNSS update of the particle filter (Fig. 3).

B. Lane Positioning Protection Level (LPPL)

This second parameter will be analogous to the protection level parameters coming from the aerial navigation, and described in [12] and will follow the equation:

$$\mathrm{LPPL} = K_{\mathrm{LPPL}} \times \sigma_{pos}$$

where K_{LPPL} can be calculated with the Rayleigh inverse cumulative distribution function (we assume two dimensions

and $\sigma = 1$) and will indicate how cautious we are when we provide a protection level:

$$K_{\mathrm{LPPL}} = Rayleigh(\sigma = 1)^{-1}(1 - P_{md})$$

being P_{md} the probability of missed detection selected. This value will be fixed according to the needs of the intended application, being for our experiments $K_{\mathrm{LPPL}} = 3.034$. The value of σ_{pos} can be estimated as the maximum eigenvalue of the covariance matrix for the position in x, y coordinates.

V. Experimental Results

Different experiments were done to test our system. In this section we present the results obtained in tests with real data collected in Berlin during a campaign of the European project CVIS (Cooperative Vehicle Infrastructure Systems) [13]. The circuit of Berlin represents well a semiurban area with some spare blockages of the GNSS coverage. In addition to the real outages, we simulated three GNSS masks of 12 s each in order to analyze the system performance in conditions of bad satellite visibility.

The test vehicle was equipped with a MEMS Analog Device gyro component and two GPS receivers, one (μBlox) using EGNOS, the other (Trimble 5700) using SAPOS network dual-frequency kinematic data (for reference). Information about the vehicle speed was collected from the CAN bus.

A. Double Integrity Indicator

As it was introduced in Section IV, in our approach two parameters are in charge of notifying when the system should not be used by an intended application. These two parameters are now illustrated in the image of Fig. 4, where the values of the integrity parameters μLO and LPPL are shown during a lane change maneuver from segment 34 (left lane) to segment 183 (right lane). In this image, the lane in which the vehicle is allocated by our algorithm is shown next to the positions of the vehicle (marked with red star), along with some extra information about the lane and its carriageway that is explained in the caption of the Fig. 4 and is also available for applications. When no GNSS updates are performed, the value of the LPPL parameter increases due to the diminution of the confidence of the filter on its output position. A larger dispersion of the particles and their weights also influences the value of the probability of lane occupancy, that becomes lower. As long as some particles lay outside the limits of segment 34, the confidence on the lane assignment must decrease. This fact is reported by the parameter μLO. As these particles are moving from lane 34 towards lane 183, they are assigned to the latter, and the probability of segment 183 increases following

$$\mu_k^{m=183} = 1 - \mu_k^{m=34}.$$

This is due to the fact that both segments 34 and 183 collect all the particles of the filter during this maneuver.

The transition between both segments has been enhanced by two edge-boxes in the image of Fig. 4. After the switch is performed, the probability of the segment 183 continues

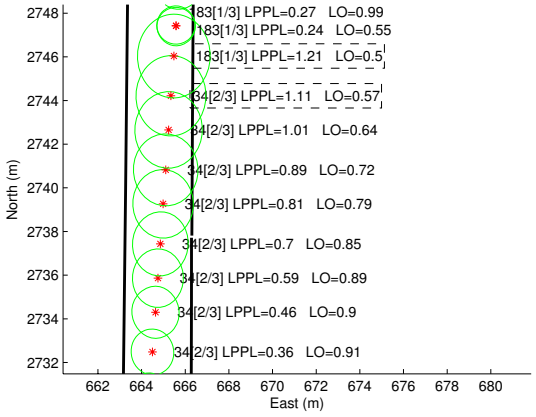

Fig. 4. Example of lane change. Solid black lines represent the median line for each lane. Information provided to the user during the maneuver: Segment ID, between squared brackets respectively the relative lateral position of the segment on the carriageway and number of lanes on the carriageway, and values of LPPL and μLO respectively. The red stars stand for the positioning outputs of the filter, while the green ellipses represent the 2σ envelope for estimated horizontal positioning errors assuming a Gaussian distribution (95% percent of fixes fall within the ellipsis).

increases (from 0.5 to 0.55). When a new GNSS position arrives, the particles and their weights are redistributed, affecting the value of LPPL and μLO. Since the confidence on the position is much higher (LPPL reaches values corresponding to a GPS/EGNOS update like 0.3 m), the dispersion of the particles is lower and μLO becomes near one (0.99). The low values of LPPL and μLO indicate a lane change carried out under good conditions for the positioning. This way, although the values of μLO are low at some instants, thanks to the LPPL indicator the overall confidence on the navigation and map-matching can be found to be high.

This example of a lane change is representative of the benefits of using a double integrity indicator. Indeed, by paying attention only at the value of the μLO parameter, it is not possible to distinguish between:

a) a situation in which the position of the vehicle is uncertain (due for example to a blockage of GNSS signals) and consequently the allocation of the vehicle on one lane is difficult, and
b) the situation of the example in which the position of the vehicle is well known anytime, and the vehicle simply drives between the lanes during a period of time.

On the other hand, using exclusively the LPPL parameter could lead to an unrealistic overconfidence on the segment matching. This would be, for instance, the case of a vehicle that drives in the middle of two lanes with good GNSS coverage. In fact, the position is accurately estimated but any application that requires high certainty on the lane assignment (e.g. lane speed control) should not be launched as the probability of the μLO parameter would result low (close to 0.5).

B. Analysis of mismatches

In our experiments there are two reasons for a mismatch in the lane assignment.

- Errors due to undetected GNSS outliers. In case of undetected GNSS outliers (undetected by means of GNSS only fault detection tests), the values of the LPPL indicator will show an unrealistic high confidence on the positioning. In this scenario two things may occur: first case is when the outlier leads to an error in the position that is found feasible by the Emap observations, and therefore the error is not detected by the integrity indicators. Against this, more efficient GNSS fault detection and exclusion (FDE) algorithms must be developed, which is out of the scope of this paper; in the second case, the Emap observations may correct the outlier if the road geometry and topology prevents from changing from one segment to another, i.e., if the lane of origin is not topologically connected to the new segment.
- Errors due to drifts of the vehicle position as a consequence of a long GNSS blockage, or a series of GNSS positions rejected in the GNSS integrity test. In this case, integrity parameters must reflect the situation, providing useful information about the actual reliability of the system.

Examples of these two cases can be found in the test scenario of Berlin. When a mismatched is caused by undetected GNSS outliers, LPPL values do not supply any information about the mismatch, while μLO values may show a diminution when it is estimated that the vehicle drives between two lanes. Setting the integrity alarms in such a way that the user would be warned in this situation would fire them also every time the vehicle realizes an intended lane change. Therefore, it is important that FDE tests are accomplished prior to positioning and map-matching.

A example of lane assignment error due to a drift of the estimated position of the vehicle in absence of GNSS coverage is shown in Fig. 5. During the long GNSS gap the estimate of the vehicle position drifts invading progressively the contiguous lane. Both parameters reflect this situation with high values of LPPL (over 5 m) and low values of μLO (close to 0.5) during the period of mismatch. Let us note that the value of μLO may be lower than 0.5 when the particles are assigned to more than two lanes, something that may happen in case of long absences of GNSS updates. In the example of Fig. 5 both LPPL and μLO show significative values, and it can be accepted that the user is warned of the unreliability of the navigation and map-matching solution.

C. Performance of Integrity Indicators

In order to assess the benefits of the integrity parameters along the complete circuit, we fixed alert limits for both μLO and LPPL parameters, $\mu\mathrm{LO}_{\mathrm{Th}}$, $\mathrm{LPPL}_{\mathrm{Th}}$, according to certain user specifications (that depend on the intended application). Final values for the thresholds were settled experimentally and fixed to $\mu\mathrm{LO}_{\mathrm{Th}} = 0.86$, and $\mathrm{LPPL}_{\mathrm{Th}}$=1.5.

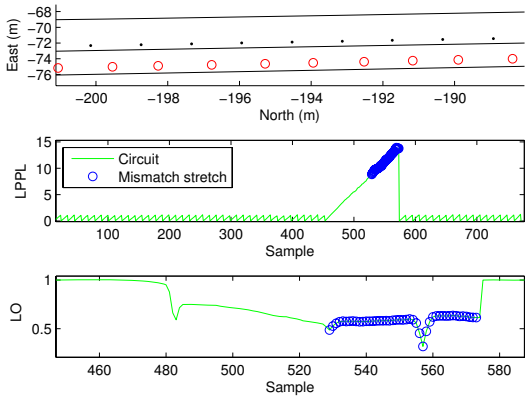

Fig. 5. (Top) A stretch of estimated vehicle trajectory during a mismatch: road lanes (solid black), ground truth (black ·), filter positions (red o). (Middle) LPPL values along a stretch of the circuit (solid green) and during the period of mismatch (blue o). (Bottom) μLO values along a stretch of the circuit (solid green) and during the period of mismatch (blue o).

TABLE I
INTEGRITY RESULTS FOR THE TESTS WITH AND WITHOUT SIMULATED GNSS MASKS.

GNSS Mask	MDR	OCDR	FAR	CMR	ECMR
No	0.0119	0.9758	0.0123	0.9873	0.9881
Yes	0.0012	0.9388	0.0600	0.9803	0.9988

The subset of values that verify the alarm area are compared to real mismatches of lane assignments. In our case we assume $\{\mu$LOA/SX $\cap$ LPPLA/SX$\}$, being μLOA/SX the subset A that verifies the condition for the scenario SX under consideration, and analogous for LPPLA/SX with LPPL. Missed detections (MD) and false alarms (FA) are then calculated. False alarm and missed detection rates (FAR and MDR respectively) can be computed by simply dividing the number of FA and MD by the total number of samples of the test. The overall correct detection rate (OCDR) follows the expression:

$$\mathrm{OCDR} = 1 - \mathrm{FAR} - \mathrm{MDR}.$$

Table I shows the values of interest collected in the experiments. Apart from the aforementioned MDR, OCDR and FAR, we found interesting to include in this Table the index of correct matches rate (CMR), that represents the rate of correct matches obtained directly from the lane assignment process, and enhanced correct matches rate (ECMR), that stands for the rate of correct matches plus wrong matches that are correctly identified. As long as the values of ECMR are higher than CMR, with final OCDR within acceptable limits, the integrity parameters are beneficial.

The following conclusions can be yielded by analyzing Table I. The fact that the ECMR value in the test with a simulated GNSS mask of more than 30 s is very close to one, and clearly higher than the CMR value in the same test shows the clear benefit of the integrity information when

coverage is poor. In the test without GNSS mask, the value of CMR is quite good, although affected by the GNSS outliers that were undetected by our Nyquist integrity test based on the Mahalanobis distance. Nevertheless, the final ECMR is higher, what shows that the information provided by the integrity parameters can be of interest also under good conditions of satellite visibility. The selection of a high value of $\mu\mathrm{LO}_{\mathrm{Th}}$ and a low value of $\mathrm{LPPL}_{\mathrm{Th}}$ (we could say that $\mu\mathrm{LO}_{\mathrm{Th}} = 0.86$, and $\mathrm{LPPL}_{\mathrm{Th}}$=1.5 are strict values) leads to higher rates of false alarms, specially in the test with long GPS gaps. The choice of the integrity thresholds always entails a risk, that can be understood as a trade-off between missed detections and false alarms. The final user application will determine their level of acceptance.

VI. CONCLUSIONS AND FUTURE WORKS

The problem of integrity provision for a map-matched position was addressed in the paper. To the best of the authors' knowledge, this is the first work that provides integrity values that represent all the sensors and map references employed in the determination of the map-matched positions.

In our approach, a single process for positioning and map-matching based on a particle filter integrates the measurements coming from a GNSS receiver, a gyroscope and the odometry of the vehicle with road information stored in an enhanced map. The Emap data about the geometry and topology of the road at the lane level are employed as observations of the filtering process. This way, positioning and map-matching appear as a common output and the vehicle is localized and allocated on the most suitable road lane.

The integrity information is based on two parameters that stand for the filter reliability on the lane assignment and the position on this lane. The results achieved in tests performed in real scenarios show how our method can model positioning and lane assignment ambiguities, informing the user when the information coming from the navigation system is not reliable.

Future works in this line will be dedicated to perform more tests for validation of the method in very different scenarios, such as rural and urban sites.

ACKNOWLEDGMENTS

This research investigation has been carried out in the frame of the European project CVIS (Cooperative Vehicle Infrastructure Systems) by researchers of LCPC (Geolocalization Group), partners of the Positioning and Mapping subproject POMA of CVIS, and the group of Intelligent Systems and Telematics/University of Murcia, awarded as an excellence researching group in frames of the Spanish Plan de Ciencia y Tecnología de la Región de Murcia (04552/GERM/06). The authors would like to thank the Spanish Comisión Interministerial de Ciencia y Tecnología and the Spanish Ministerio de Fomento for their support under the grants TIN2008-06441-C02-02 and FOM/2454/2007 respectively.

Finally, the authors thanks go also to Marius Schingelhof and his team at DLR (German Aerospace Center), Institute of Transportation Systems, for their work in the data collection of Berlin.

REFERENCES

[1] D. Obradovic, H. Lenz, and M. Schupfner, "Fusion of sensor data in Siemens car navigation system", *IEEE Transactions on Vehicular Technology*, vol. 56, pp. 43–50, Jan. 2007.

[2] SafeSpot European Project. "Cooperative vehicles and road infrastructure for road safety". *http://www.safespot-eu.org*

[3] R. Toledo-Moreo, J. Santa, M.A. Zamora-Izquierdo, B. Bubeda, A.F. Gomez-Skarmeta, "A Study of Integrity Indicators in Outdoor Navigation Systems for Modern Road Vehicle Applications". *IROS 2008 2nd Workshop on Planning, Perception and Navigation for Intelligent Vehicles*. 2008.

[4] D. Bétaille, R. Toledo-Moreo, J. Laneurit. "Making an Enhanced Map for Lane Location Based Services". *In Proceedings of the 11th International IEEE Conference on Intelligent Transportation Systems* Beijing, China, October 12-15. pp. 711–716, 2008.

[5] K. Wevers and S. Drehers. "Digital Maps for Lane Level Positioning". *In Proceedings of the 15th ITS World Congress*. paper nb 20487. New York, USA, November, 2008.

[6] S. Shroedl, S. Rogers, C. Wilson, "Map refinement from GPS traces". DaimlerChrysler Res. and Technol. North America, Palo Alto, CA, RTC Rep. No. 2000/6, 2000.

[7] O. Le Marchand, P. Bonnifait, J. Ibañez-Guzmán, F. Peyret, D. Bétaille, "Performance Evaluation of Fault Detection and Exclusion Algorithms as Applied to Automotive Localisation", *In Proc. of the European Navigation Conference GNSS*, Toulouse, France, Apr. 2008.

[8] R. Toledo-Moreo, M.A. Zamora-Izquierdo, B. Ubeda-Miarro, A.F. Gomez-Skarmeta, High-Integrity IMM-EKF-Based Road Vehicle Navigation With Low-Cost GPS/SBAS/INS, *IEEE Transactions on Intelligent Transportation Systems*, vol. 8, no. 3, 2007, pp. 491–511.

[9] M.A. Quddus W.Y. Ochieng , R.B. Noland,"Integrity of map-matching algorithms". Elsevier Transportation Research Part C 14 283302, 2006.

[10] Eidehall A., Tracking and threat assessment for automotive collision avoidance. Phd Thesis. Linköping, Sweden. 2007.

[11] R. Toledo-Moreo, D. Bétaille, F. Peyret, J. Laneurit "Fusing GNSS, Dead-reckoning and Enhanced Maps for Road Vehicle Lane-Level Navigation". *Journal of Selected Topics in Signal Processing*, (to be printed), 2009.

[12] Minimum Operational Performance Standards For Global Positioning System/Wide Area Augmentation System Airborne Equipment. RTCA, RTCA/DO-229C November 28, 2001 Supersedes DO-229B. 2001

[13] Cooperative Vehicle Infrastructure Systems. European Project of the 6th Framework Program. www.cvisproject.org